

# The eccentricity of binaries detectable in gravitational waves

I. Kowalska<sup>1</sup>, T. Bulik<sup>1,2</sup>, K. Belczynski<sup>1,3</sup>, M. Dominik<sup>1</sup>, and D. Gondek-Rosinska<sup>4,2</sup>

<sup>1</sup> Astronomical Observatory, University of Warsaw, Al Ujazdowskie 4, 00-478 Warsaw, Poland

<sup>2</sup> Nicolaus Copernicus Astronomical Center, Bartycka 18, 00716, Warsaw, Poland

<sup>3</sup> Dept. of Physics and Astronomy, University of Texas, Brownsville, TX 78520, USA

<sup>4</sup> Institute of Astronomy, University of Zielona Góra, ul. Lubuska 2, 65-265 Zielona Góra, Poland

Received ; accepted

## ABSTRACT

**Context.** The current gravitational wave detectors have reached their operational sensitivity and are nearing detection of compact object binaries. In the coming years we expect that the Advanced LIGO/VIRGO will start taking data. At the same time there are plans for third generation ground based detectors like the Einstein Telescope, and space detectors like DECIGO.

**Aims.** We discuss the detectability of eccentricity of inspiral compact object binaries with the use of their gravitational wave signal. We analyze the expected distributions of eccentricities and calculate the fraction of binaries with detectable eccentricity.

**Methods.** We use the StarTrack binary population code to investigate the properties of the population of compact binaries at formation. We evolved their orbits until the point they enter a given detector sensitivity window and analyze the distribution of eccentricity at that time.

**Results.** We find that in the case of NS-NS binaries a small fraction (0.53%) should have eccentricities detectable with the Advanced LIGO/VIRGO. This fraction increases for the planned Einstein Telescope (ET) and reaches 2.98%, while for the DECIGO type detectors the majority (68.11%) of NS-NS binaries shall have detectable eccentricities. In the case of BH-NS fraction of detectable binaries with non-zero eccentricities for Advanced LIGO/VIRGO, ET and DECIGO are equal to 0.15%, 1.16% and 15.99%, respectively. For BH-BH binaries the fraction of objects with detectable eccentricities is very small - in Advanced LIGO/VIRGO it's dropping to zero, while for ET and DECIGO it's equal to 0.62% and 2.49%, respectively.

**Key words.** binaries – gravitational waves

## 1. Introduction

As the interferometric gravitational wave detectors LIGO and VIRGO (Harry & the LIGO Scientific Collaboration 2010; Acernese et al. 2006) have reached the design sensitivities the first detection of gravitational wave is getting closer. Both detectors will undergo serious improvements to increase the sensitivity (Smith & LIGO Scientific Collaboration 2009; Spallicci et al. 2005).

It is therefore important to investigate the properties of the primary candidate sources for detection, namely compact object binaries. There have been a number of papers dealing with several properties of the population of compact binaries (e.g., Nelemans & van den Heuvel 2001; Voss & Tauris 2003; De Donder & Vanbeveren 2004; Sipior & Sigurdsson 2002; Pfahl et al. 2005; Dewi et al. 2002, 2005; Bogomazov et al. 2007; Kiel et al. 2010). In particular, Abadie et al. (2010) presented estimated detection rates. Also the mass spectrum (Gondek-Rosińska et al. 2007), and even spin properties (Schnittman 2004; Mandel & O'Shaughnessy 2010) had been studied. In this paper we will present yet another aspect of the merging compact object binary population: the distribution of eccentricity.

Currently we know from the radio observations only 6 compact object binaries with merger times below the Hubble time - all of them NS-NS (neutron star - neutron star) systems, and we do not know any BH-NS (black hole - neutron star) nor BH-BH (black hole - black hole) system. The known NS-NS systems are listed along with their orbital parameters in Table 1. The observations represent preferably the population of the long lived

NS-NS. However, it has been suggested that a significant fraction of the population of the merging NS-NS may originate in the so called ultra-compact NS-NS binaries, with much shorter merger times (Belczynski et al. 2002a). Besides, the small number of the known pulsars allows for a significant fraction of very eccentric binaries.

As no BH-NS nor BH-BH binaries are known we can only relay on the evolutionary considerations when estimating their number and properties. It has been found that their number depends very strongly on the outcome of the common envelope phase when the secondary is on the Hertzsprung gap. This phase will very likely end up as a merger with formation of Thorne Zytkov object. However, it was recently demonstrated that in low metallicity environment the common envelope mergers may be (to some extent) avoided and the BH-BH formation is very effective (Belczynski et al. 2010b).

Potentially, eccentricity of a compact object binary may be derived from analysis of the inspiral signal, provided that the eccentricity is significant. In this paper we investigate the detectability of eccentricity in the currently working and in the future detectors. For the currently working detectors (LIGO and VIRGO) we assume that the sensitivity of the detectors will allow to measure the signal for the frequencies starting at 30 Hz. This may not be accurate for the current state of these instruments, however it does well represent the predicted sensitivity of the Advanced LIGO/VIRGO detectors. We consider two future detectors: the Einstein telescope (Van Den Broeck 2010) and DECIGO (Kawamura 2006; Seto et al. 2001). For the Einstein telescope we assume that binaries shall be detectable from 3 Hz,

and for DECIGO we assume that the lowest frequency detectable is 0.3 Hz. In all cases these have to be treated as indicative numbers that roughly describe these instruments.

We also investigate the properties of the population of compact objects and show the fraction for each detector with detectable eccentricity. In section 2 we describe the model used to investigate the population of compact object binaries, and discuss the detectability of eccentricity with gravitational wave observations. Section 3 contains the results for the current and future gravitational wave detectors. In section 4 we summarize and discuss the results.

## 2. The model

### 2.1. Compact object binary population model

In order to model the population of compact object binaries we used the *StarTrack* population synthesis code (Belczynski et al. 2002b) to perform a suite of Monte Carlo simulations of the stellar evolution of stars in environments of two typical metallicities:  $Z = Z_{\odot} = 0.02$  and  $Z = 10\% Z_{\odot} = 0.002$  (e.g., Belczynski et al. 2010b). In these calculations we employ the recent estimates of mass loss rates (Belczynski et al. 2010a). We calculate a population of 2 million massive binary stars, tracking the ensuing formation of relativistic binary compact objects: double neutron stars (NS-NS), double black hole binaries (BH-BH), and mixed systems (BH-NS). Our modeling utilizes updated stellar and binary physics, including results from supernova simulations (Fryer & Kalogera 2001) and compact object formation (Timmes et al. 1996), incorporating elaborate mechanisms for treating stellar interactions like mass transfer episodes (Belczynski et al. 2008) or tidal synchronization and circularization (Hut 1981). We put special emphasis on the common envelope evolution phase (Webbink 1984), which is crucial for close double compact object formation as the attendant mass transfer allows for efficient hardening of the binary. This orbital contraction can be sufficiently efficient to cause the individual stars in the binary to coalesce and form a single highly rotating object, thereby aborting further binary evolution and preventing the formation of a double compact object. Because of significant radial expansion, stars crossing the Hertzsprung gap (HG) very frequently initiate a common envelope phase. HG stars do not have a clear entropy jump at the core-envelope transition (Ivanova & Taam 2004); if such a star overflows its Roche lobe and initiates a common envelope phase, the inspiral is expected to lead to a coalescence (Taam & Sandquist 2000). In particular, it has been estimated that for a solar metallicity environment (e.g., our Galaxy), properly accounting for the HG gap may lead to a reduction in the merger rates of BH-BH binaries by  $\sim 2 - 3$  orders of magnitude (Belczynski et al. 2007). In contrast, in low metallicity environment this suppression is much less severe ( $\sim 1$  order of magnitude; Belczynski et al. (2010b)). The details of the common envelope phase are not yet fully understood, and thus in what follows we consider two set of models, one which does not take into account the suppression (optimistic models: marked with A), and set that assumes the maximum suppression (pessimistic models: marked with B). Solar metallicity and 10% of Solar metallicity are marked with Z and z, respectively. In case of NSs we adopt natal kick distributions from observations of single Galactic pulsars (Hobbs et al. 2005) with  $\sigma = 265$  km/s. However for BHs we draw kicks from the same distribution but with the lower magnitude: inverse proportional to the amount of fall back expected at the BH formation (e.g., Fryer & Kalogera 2001). In particular, for most massive

BHs that form with the full fall back (the direct BH formation) the magnitude of natal kick is zero. Additionally we test one more set of models in which the magnitude of NS kicks is decreased by factor of 2:  $\sigma = 132.5$  km/s, as some observations and empirically based arguments seem to indicate that natal kicks in close binaries are lower than for single stars (Dessart et al. 2006; Kitaura et al. 2006). The BH kicks are decreased in the similar fashion as in models with the full NS kicks. Standard value of  $\sigma$  parameter is denoted by K and smaller value by k. Detailed list of models considered in this paper is presented in Table 2. Model AZK is a standard set of parameters described in detail by Belczynski et al. (2002b).

**Table 2.** The list of models of stellar evolution used in the paper.

Model	Metallicity	$\sigma$ [ $\text{km s}^{-1}$ ]	HG
AZK	$Z_{\odot}$	265.0	+
BZK	$Z_{\odot}$	265.0	-
Azk	$Z_{\odot}$	132.5	+
Bzk	$Z_{\odot}$	132.5	-
AzK	10% $Z_{\odot}$	265.0	+
BzK	10% $Z_{\odot}$	265.0	-
Azk	10% $Z_{\odot}$	132.5	+
Bzk	10% $Z_{\odot}$	132.5	-

### 2.2. Evolution of orbits

The evolution of the orbit of compact object binary under the influence of gravitational radiation had been calculated by (Peters & Mathews 1963; Peters 1964). In the quadrupole approximation the orbit decays as:

$$\frac{da}{dt} = -\frac{\beta}{a^3} \Psi(e) \quad \Psi(e) = \frac{1 + 73/24e^2 + 37/96e^4}{(1 - e^2)^{7/2}} \quad (1)$$

where  $a$  is great semi-axis,  $e$  is eccentricity of binary,  $M_1$  is mass of the first component,  $M_2$  is mass of second component and

$$\beta = \frac{64}{5} \frac{G^3 \mu M^2}{c^5} \quad \mu = \frac{M_1 M_2}{M_1 + M_2} \quad (2)$$

While the eccentricity decays as:

$$\frac{de}{dt} = -\frac{19}{12} \frac{\beta}{a^4} \Phi(e) \quad \Phi(e) = \frac{(1 + 121/304e^2)e}{(1 - e^2)^{5/2}} \quad (3)$$

Using the above formulas we can express gravitational wave frequency as a function of eccentricity:

$$f_{GW}(e) = \frac{G^{1/2} M_1 + M_2^{1/2}}{\pi} \frac{(1 - e^2)^{3/2}}{c_0^{3/2} e^{18/19}} [1 + \frac{121}{304} e^2]^{-1305/2299} \quad (4)$$

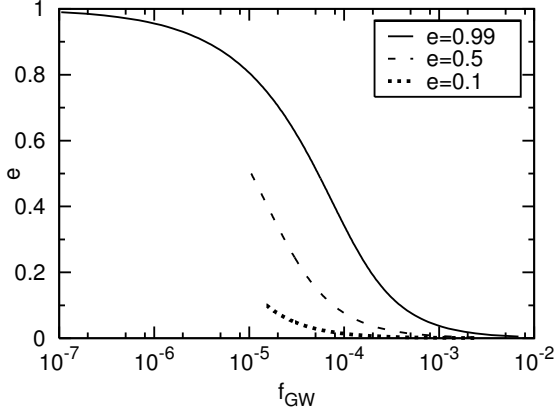
where  $c_0 = \frac{a_0(1-e_0^2)}{e_0^{12/19}} [1 + \frac{121}{304} e_0^2]^{-1305/2299}$

It is worth noting that  $f_{GW}(e)$  is only the first non-zero harmonic, where gravitational wave frequency is twice the orbital frequency (i.e.,  $f_{GW} = \frac{2}{P_{orb}}$ ).

We present the evolution of eccentricity as a function of gravitational wave frequency in Figure 1 for binary neutron star

**Table 1.** Known merging compact object binaries

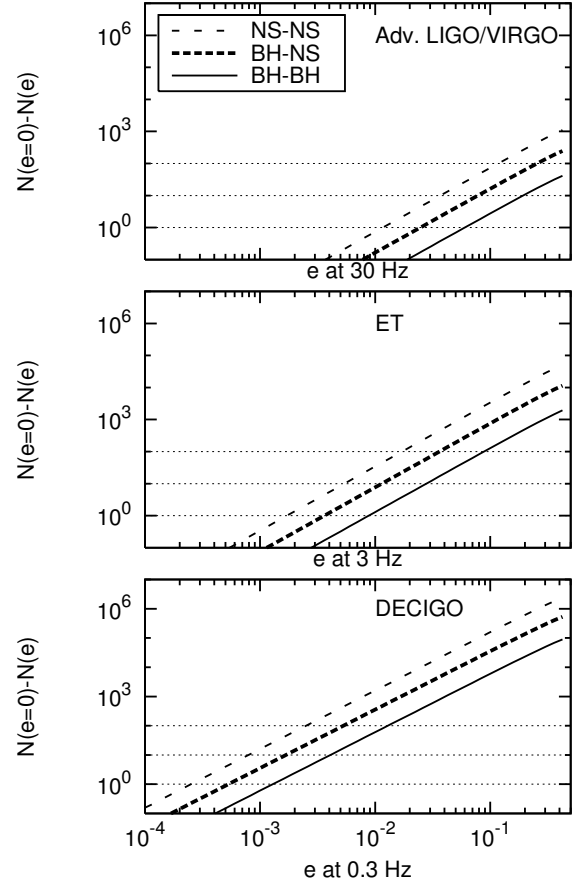
Name	$P_{orb}$ [h]	Present $e$	$T_{merge}$ [Gyr]	$e$ at 0.3 Hz	$e$ at 3 Hz	$e$ at 30 Hz	Ref.
J0737-3039A/B	2.454	0.088	0.085	$4.5 \times 10^{-5}$	$4 \times 10^{-6}$	$3.5 \times 10^{-7}$	Burgay et al. (2003)
B2127+11C	8.05	0.681	0.2	$2.9 \times 10^{-4}$	$2.6 \times 10^{-5}$	$2.3 \times 10^{-6}$	Anderson et al. (1990)
J1906+0746	3.98	0.085	0.3	$2.6 \times 10^{-5}$	$2.3 \times 10^{-6}$	$2 \times 10^{-7}$	Lorimer et al. (2006)
B1913+16	7.752	0.617	0.3	$2.2 \times 10^{-4}$	$1.9 \times 10^{-5}$	$1.7 \times 10^{-6}$	Weisberg & Taylor (2005)
J1756-2251	7.67	0.181	1.7	$2.6 \times 10^{-5}$	$2.5 \times 10^{-6}$	$2.2 \times 10^{-7}$	Faulkner et al. (2005)
B1534+12 (=J1537+1155)	10.098	0.274	2.7	$3.6 \times 10^{-5}$	$3.2 \times 10^{-6}$	$2.8 \times 10^{-7}$	Wolszczan (1991)

**Fig. 1.** We present 3 cases of eccentricity evolution, starting with  $e_0 = 0.99$ ,  $a_0 = 216.2235 R_\odot$  (solid line),  $e=0.5$ ,  $a_0 = 10.048 R_\odot$  (long dashed line) and  $e=0.01$ ,  $a_0 = 7.8428 R_\odot$  (short dashed line). Initial orbital separation is chosen such that binary will merge within time  $T_{merge} = 10$  Gyr in each case.

with equal masses of  $1.4 M_\odot$ . Initial frequency corresponds to great semi-axis such as the merger time is set at  $T_{merge} = 10^4$  Myr. We show three different cases of initial eccentricity:  $e = 0.99$ ,  $e = 0.5$ ,  $e = 0.01$ .

### 2.3. Detectability of eccentricity

In this section we address the question of detectability of small eccentricity with gravitational wave detectors. The effect of eccentricity will be detectable once it influences the waveform significantly. A simple way of estimating this effect is to count the number of cycles that a given source stays in a detectors sensitivity range. A signal from merging source will enter the detectors sensitivity window at low frequencies and stay there until the coalescence. We consider three cases: a double neutron star binary consisting of the neutron stars with the mass of  $1.4 M_\odot$ , a black hole neutron star binary with the masses of  $10$  and  $1.4 M_\odot$ , and a binary black hole with equal masses of  $10 M_\odot$ . We are interested in the change in number of cycles that the eccentricity induces. In Figure 2 we plot the difference between the number of cycles in a detector for an eccentric binary and for the circular binary. The three panels correspond to three different frequencies at which a binary becomes detectable. We assume that non-zero eccentricity can be detected if the difference in number of cycles introduced by non-zero eccentricity over the circular binary is larger than some threshold. In this paper we consider three different thresholds, namely 1, 10 and 100. We calculate number of orbits in quadrupole approximation by integrating frequency depending on time:

**Fig. 2.** The differences in number of cycles between the lower part of the sensitivity window and coalescence for three detectors with low frequency threshold of 0.3 Hz - bottom panel, 3 Hz - panel in the middle, and 30 Hz - top panel. The three lines correspond to double neutron star binaries (dashed line), black hole neutron star binaries (short dashed line) and double black hole binaries (solid line). Horizontal dotted lines represent difference of 1, 10 and 100 orbits.

$$N_{orb} = \int_{f_{lim}}^{f_{isco}} f(t) dt \quad (5)$$

where  $f_{lim}$  is characteristic frequency for each detector (30 Hz for Advanced LIGO/VIRGO, 3 Hz for ET and 0.3 Hz for DECIGO) and  $f_{isco}$  is frequency at innermost stable circular orbit:

$$f_{isco} = \frac{c^3}{6\sqrt{6}G(M_1 + M_2)} \quad (6)$$

For the Advanced LIGO/VIRGO type detectors this means that minimum detectable eccentricity of a double neutron star binary must be  $e(30 \text{ Hz}) > 1.35 \times 10^{-2}$ , while for future detectors these limits are  $e(3 \text{ Hz}) > 1.89 \times 10^{-3}$  for ET-like detector, and  $e(0.3 \text{ Hz}) > 2.64 \times 10^{-4}$  for the DECIGO like one. In the case of more massive binaries these limits become higher because more massive binaries have lower frequencies at coalescence and are detectable for smaller number of cycles. For the mixed black hole neutron star binary the limits are  $e(30 \text{ Hz}) > 2.61 \times 10^{-2}$ ,  $e(3 \text{ Hz}) > 3.65 \times 10^{-3}$ , and  $e(0.3 \text{ Hz}) > 6.0 \times 10^{-4}$ . Finally, in the case of binary black holes the eccentricity will be detectable if it is  $e(30 \text{ Hz}) > 6.98 \times 10^{-2}$ ,  $e(3 \text{ Hz}) > 9.76 \times 10^{-3}$ , and  $e(0.3 \text{ Hz}) > 1.36 \times 10^{-3}$ . For detail see Table 3.

The limits presented above are certainly very optimistic. If we take as a threshold difference of 10 or 100 orbits minimum detectable eccentricity is higher. In consequence number of expected binaries is decreasing. For pessimistic threshold (equal 100) minimum detectable eccentricity for all types of binaries is of the order of magnitude higher than in the case of threshold equal to 1 orbit. For more detail see Table 4 containing limits and expected fraction of detectable binaries for threshold equal to 10 and Table 5 for threshold equal to 100.

We have computed the expected eccentricities of the known double neutron star systems - they are shown in Table 1. These values are much smaller than the detectability limits shown above.

### 3. Results

#### 3.1. Properties of the binaries at formation time

We start with an initial population obtained with the StarTrack code. We present the properties of the population of compact object binaries in Figure 3 - 5 in the space spanned by the initial eccentricity and initial gravitational wave frequency (twice the orbital frequency). Each panel in these figures corresponds to a different model labeled as listed in Table 2.

The case of the NS-NS systems is shown in Figure 3. The boundary of the region populated by the systems on the left hand side corresponds to the requirement that we only present binaries that merger within the Hubble time. The bulk of the binaries shown in each panel corresponds to binaries that have undergone one CE phase in their evolution. The top row corresponds to the models AZK, AZk, AzK, and Azk, in which we allow the binaries to cross through the common envelope with the donor on Hertzsprung Gap, denoted by "+" in Table 2. These binaries may undergo a second common envelope phase with a Helium star companion. At the second CE stage the orbit is tightened even more and that leads to formation of the stripe in the diagram stretching up from  $f_{GW} \approx 10^{-2} \text{ Hz}$  at  $e = 0$ . In these models the initial distribution in the space of gravitational wave frequency versus eccentricity is bimodal. The influence of the value of the kick velocity has a small impact on the shape of distributions presented in Figure 3.

In the case of BH-NS, Figure 4, and BH-BH binaries, Figure 5, we present the results of six out of eight models, since in models BZK and BZk, almost no binaries are formed in our simulations that involved  $2 \times 10^6$  initial binaries. For BH-NS and BH-BH binaries the formation of ultra-compact binaries is

not expected. The formation of NS-NS ultra-compact systems on the very close orbits is the consequence of the final CE episode initiated by a low mass Helium ( $2-4 M_\odot$ ) star and its NS companion ( $1.3 M_\odot$ ). Since the donor is about twice as massive as its companion, the CE phase is initiated and the orbit is significantly decreased in size. In case of more massive BH-BH/BH-NS binaries Helium stars are on average more massive ( $M > 3 - 4 M_\odot$ ) and they do not expand (so no CE phase), and even if low mass Helium star forms then its companion is a BH ( $M > 3 M_\odot$ ) so most likely instead of CE the RLOF is stable and does not lead to the orbital decay (mass ratio  $\sim 1$ ). Only very few systems (e.g., models AzK or Azk) produce ultra-compact BH-NS/BH-BH binaries for very special cases of binary evolution. In the case of BH-BH binaries, shown in Figure 5 we also present only six models, since models BZK and BZk do not lead to formation of BH-BH binaries (Belczynski et al. 2007). In all models there is an enhanced density of systems formed with  $e \approx 0.1$  at approximately  $10^{-5} \text{ Hz} < f_{GW} < 10^{-4} \text{ Hz}$ . In these systems the second black hole formed via direct collapse. When treating the direct collapse we assume that 10% of the mass escapes in the form of neutrinos and possibly gravitational waves. Hence the gravitational mass of the BH is 10% smaller than the baryon mass of the collapsing star. This introduces a small eccentricity  $\approx 0.1$  since the systems were circularized in the mass transfer prior the collapse and the formation of the second BH.

#### 3.2. Eccentricity when binary enters detector band

From the point of view of detection of gravitational waves it is important to know the eccentricity of a binary at the time it enters the sensitivity window of the detector. We consider three cases that approximately correspond to three types of detectors. In Figure 6 we show the distributions of eccentricity at 30 Hz, corresponding approximately to the Advanced LIGO/VIRGO detectors. In Figure 7 eccentricity at 3 Hz are shown which correspond to the case of the ET detector, and in Figure 8 we show the distribution of eccentricity at 0.3 Hz, which is the case of DECIGO detector.

The shape of distributions of eccentricity at the moment binary enters the given detector band follows automatically from the corresponding initial distribution. However one must note that for each type of binaries there is a different natural timescale and frequency, because of different mass scale of each binary. In the case of NS-NS binaries shown in the top panel of Figure 6 at 30 Hz, the distribution is either centered on the  $e \approx 10^{-6}$  for the case of models BZK, BZk, BzK, and Bzk, where we do not allow formation of ultra-compact binaries in a second CE phase. The remaining models: AZK, AZk, AzK, and Azk, show another component centered roughly at  $e \approx 10^{-4}$ . This comes from the ultra-compact binaries that went through two episodes of mass transfer in their evolutionary history and were already very tight at the second supernova explosion. The mixed BH-NS binaries, shown in the middle panel of Figure 6 exhibit a distribution of eccentricity centered at  $e \approx 3 \times 10^{-7}$ , while the eccentricity BH-BH binaries at 30 Hz, shown in the bottom panel of Figure 6 lie between  $e \approx 3 \times 10^{-8}$  and  $e \approx 3 \times 10^{-6}$ . These values of eccentricity are consistent with  $e = 0$  and in the case of Advanced LIGO/VIRGO type detectors we can safely assume that all BH-NS and BH-BH binaries are circular without any loss of sensitivity.

We present the fraction of binaries with detectable eccentricity in Table 3. For the case of NS-NS binaries there is a small tail of binaries that might have detectable eccentricity. This fraction varies from 0.14% for model AZk, to 1.87% for

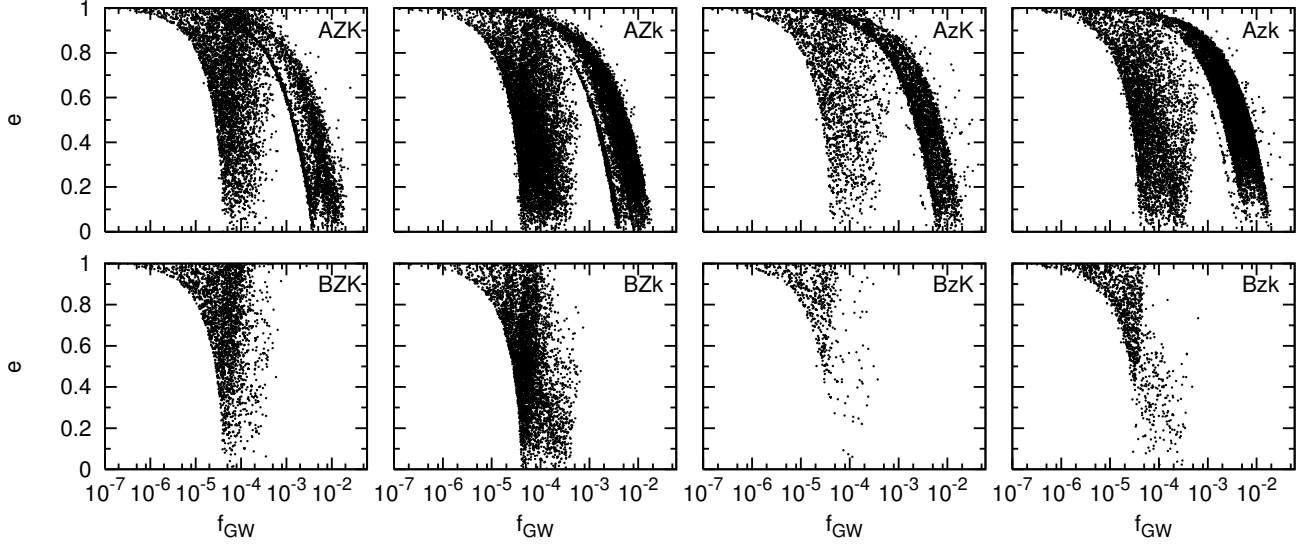


**Fig. 3.** The properties of the population of double neutron stars obtained using the StarTrack code. The plot shows only the binaries that will merger within the Hubble time.

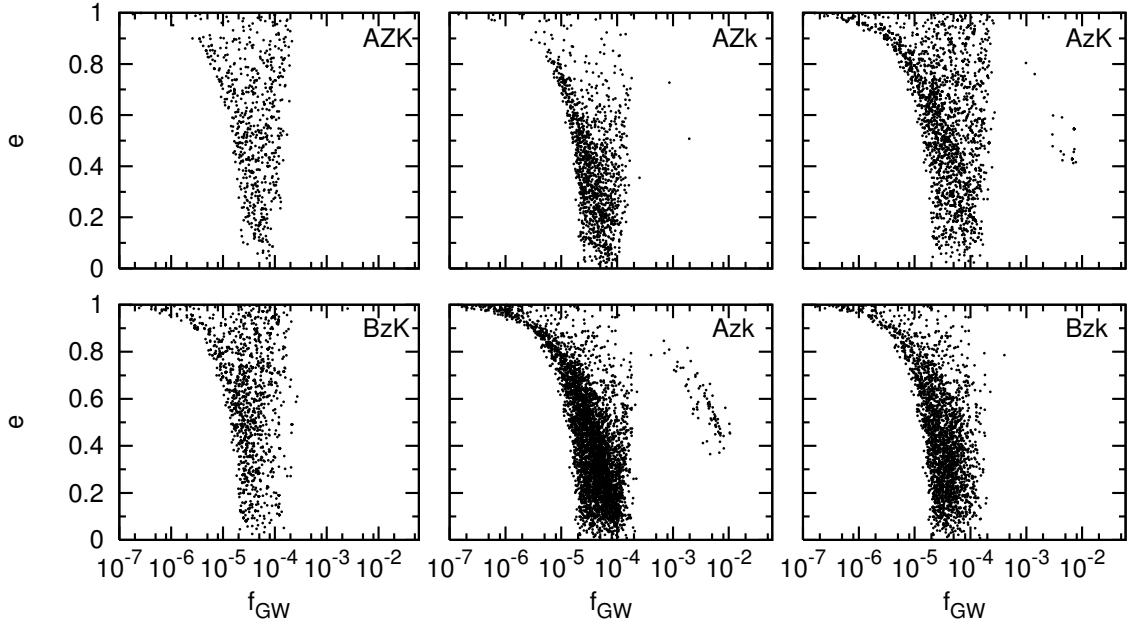


**Fig. 4.** The properties of the population of neutron star - black hole systems obtained using the StarTrack code. The plot shows only the binaries that will merger within the Hubble time.

model BzK. Given the expected rates of NS-NS binaries in Advanced LIGO/VIRGO (Abadie et al. 2010), there is a small chance of detecting a slightly eccentric binary in these detectors - see Table 7. On the other hand using of templates calculated with the assumption of  $e = 0$  is totally justified and does not lead to any significant loss of sensitivity in current ground-based detectors (Brown & Zimmerman 2010). Although in Advanced LIGO/VIRGO and ET neglecting eccentricity greater than  $e \approx 0.05$  may lead to significant loss of sensitivity (Cokelaer & Pathak 2009).

The distributions of eccentricity at 3 Hz, approximately corresponding to the case of ET are shown in Figure 7. The shape of the distributions is similar as in the Figure 6. The NS-NS eccentricity are centered on  $e \approx 10^{-5}$  for the case of models BZK,

BZk, BzK, and Bzk; in models AZK, AZk, AzK, and Azk there is an additional component centered around  $e \approx 10^{-3}$ . The expected fraction of NS-NS binaries with detectable eccentricity is somewhere between  $\approx 2\%$  from model AZk, and  $4\%$  for model BzK, see Table 3. On the other hand given the expected range of ET for NS-NS binaries one can expect that it will be able to detect at least thousands of NS-NS binaries annually. That may lead to detecting a significant number of eccentric binaries which may allow for study of the distribution of eccentricity. However, distinguish between models with and without the second CE episode will not be possible with ET, since differences in the distribution of eccentricity appear below  $e = 1.89 \times 10^{-3}$  which is our estimated threshold for detectability of eccentricity at 3 Hz. The distributions of expected eccentricity for BH-NS

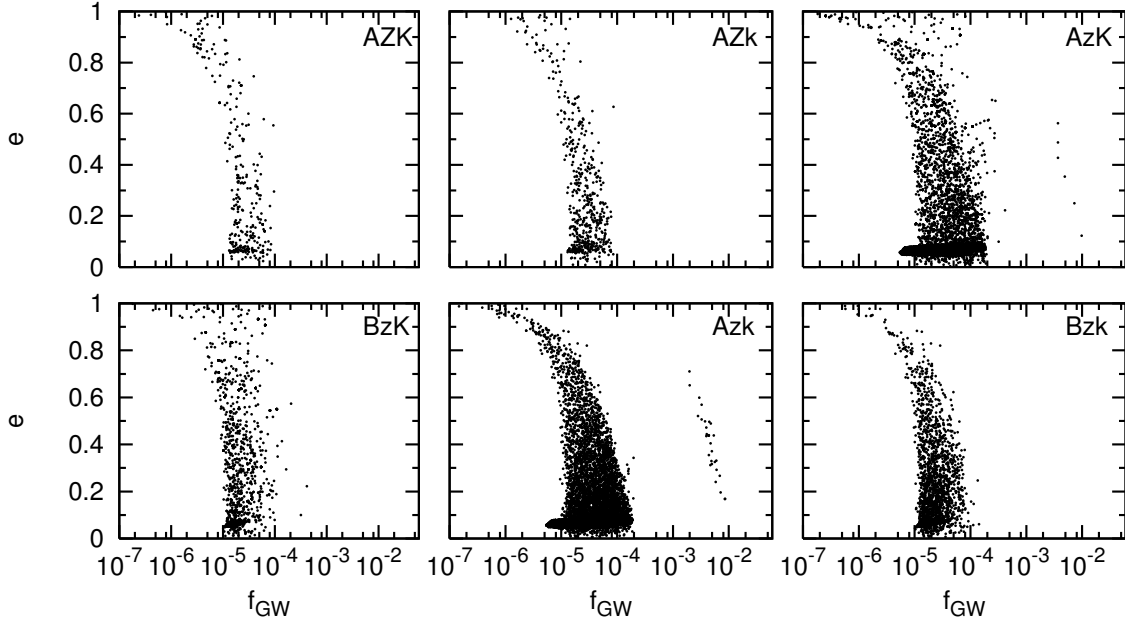


**Fig. 5.** The properties of the population of double black holes obtained using the StarTrack code. The plot shows only the binaries that will merger within the Hubble time.

binaries is shown in the middle panel of Figure 7. The distributions are rather model independent and centered below  $e \approx 10^{-5}$ . The fraction of detectable binaries is small, see the middle panel of Table 3. In one case - model BZk, it formally reaches 0.69%, however this fraction is based on just a single case. This means that using the assumption of circular templates is fully justified and lead to minimal loss of detecting power for BH-NS binaries in the case of ET. However detecting a small fraction of eccentric systems may be an interesting exercise in data analysis. The distribution of expected eccentricity of BH-BH binaries at 3 Hz is shown in the bottom panel of Figure 7. The eccentricity lie primarily in the range between  $e \approx 10^{-7}$  and  $e \approx 10^{-5}$ . The expected fraction of binaries with detectable eccentricity is very small. The highest fraction of 0.6% obtained for model AZK is based only on two cases, so our simulations were too small to effectively distinguish it from zero. Thus in the case of ET all BH-BH binaries can be treated as circular.

The distribution of expected eccentricity at 0.3 Hz is shown in Figure 8. The top panel corresponds to the case of NS-NS binaries. The shape of the distribution is similar as in the two previous cases, and the lower peak of the distributions lies at  $e \approx 10^{-4}$ , while the upper peak is centered on  $e \approx 10^{-2}$ . In this case, however, the threshold for detectability of eccentricity is at  $e = 2.6 \times 10^{-4}$ . Thus DECIGO like detectors should be able to detect quite a number of eccentric NS-NS binaries. This is shown in the bottom panel of Table 3. The fraction of NS-NS binaries with detectable eccentricity is above 25% and even above 50% for 6 out of 8 models. Thus eccentricity will be detectable for most of the NS-NS binaries observable by DECIGO. In the data analysis for those detector one will need to use templates that take into account the eccentricity. Moreover, such detectors will be able to test the presence or absence of the peak in the distribution at  $e \approx 10^{-2}$ , and directly test the evolutionary scenario that leads to formation of ultra-compact NS-NS binaries. The distribution of eccentricity for BH-NS binaries at 0.3 Hz is shown in the middle panel of Figure 8. It is centered below  $e \approx 10^{-4}$ , thus only the high eccentricity tail of the distribu-

tion will be detectable. The expected fraction of BH-NS binaries with detectable eccentricity is shown in bottom panel of Table 3. The fraction varies from a few to a few tens of percent, however the largest values are poorly determined in our simulations because of small number of systems. The fraction of detectable eccentric systems correlates with magnitude of kick velocity of newly born NS as naturally expected (large kicks impart high eccentricities or disrupt binaries). Finally, the bottom panel of Figure 8 shows the distribution of eccentricity of BH-BH binaries at 0.3 Hz. most of these systems lies between  $e \approx 10^{-6}$  and  $e \approx 10^{-4}$ . The fraction of binaries with eccentricity large enough to be detected reaches 3% for model BzK, and remains lower for the remaining models. Thus from the data analysis point of view the eccentricity of BH-BH binaries can be neglected, however detection of an eccentric BH-BH binary may be possible with DECIGO type observatory.

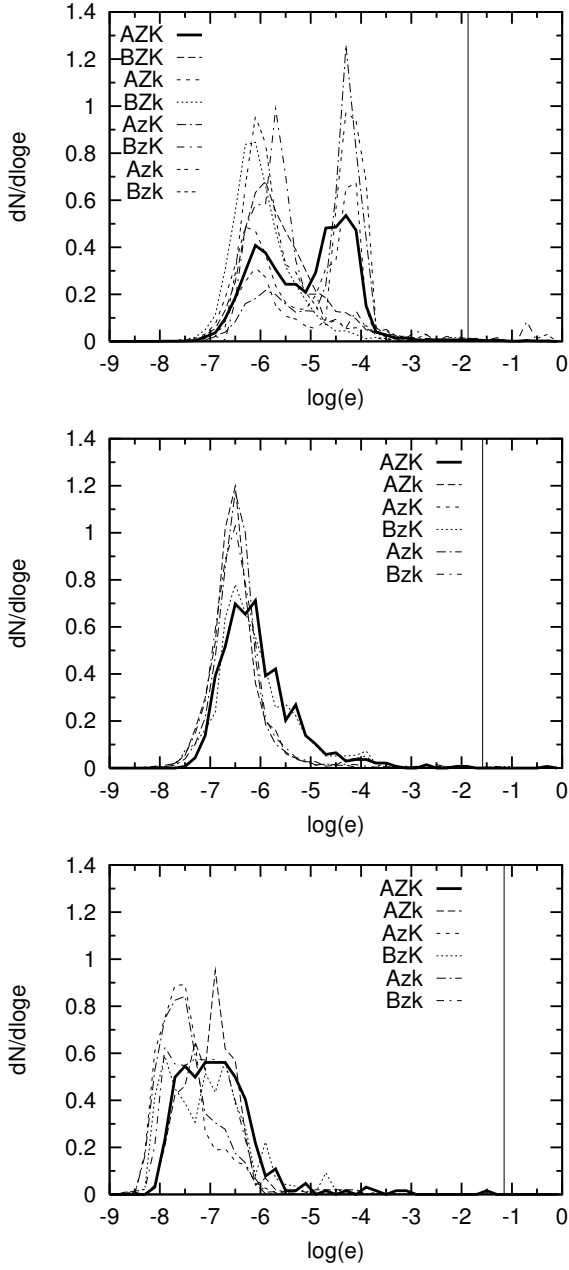


**Fig. 6.** Distribution of eccentricity for (NS-NS - top panel, BH-NS middle panel and BH-BH bottom panel) seen at 30 Hz (Advanced LIGO/VIRGO-like detectors). Solid thick line corresponds to standard model (AZK). Dashed and dotted lines shows other models. Vertical solid line shows minimal detectable eccentricity for difference in orbits equal to 1

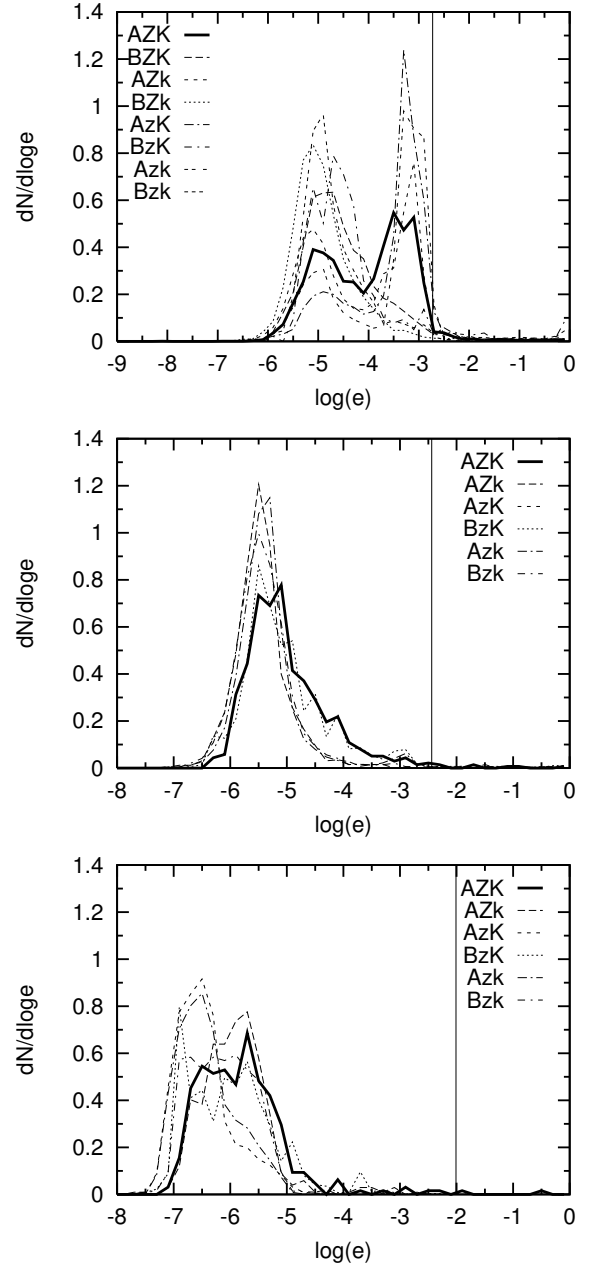


**Fig. 7.** Distribution of eccentricity for (NS-NS - top panel, BH-NS middle panel and BH-BH bottom panel) seen at 3 Hz (ET-like detectors). Solid thick line corresponds to standard model (AZK). Dashed and dotted lines shows other models. Vertical solid line shows minimal detectable eccentricity for difference in orbits equal to 1

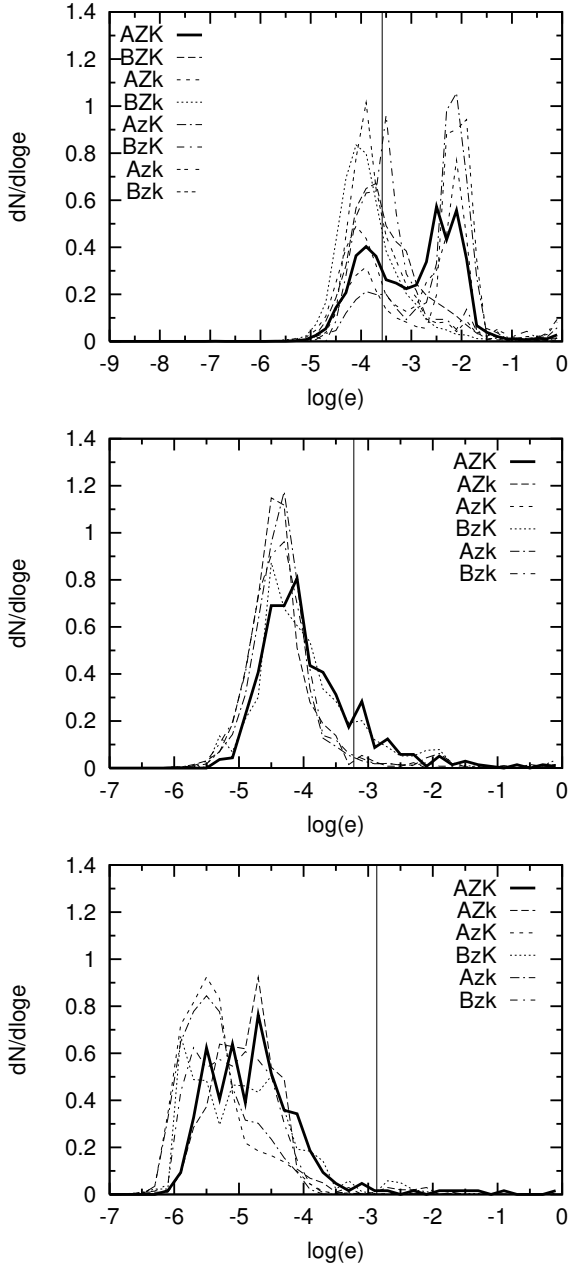


**Fig. 8.** Distribution of eccentricity for (NS-NS - top panel, BH-NS middle panel and BH-BH bottom panel) seen at 0.3 Hz (DECIGO -like detectors). Solid thick line corresponds to standard model (AZK). Dashed and dotted lines shows other models. Vertical solid line shows minimal detectable eccentricity for difference in orbits equal to 1

**Table 3.** Percent of the compact binaries that should be detectable in future interferometers. Top table correspond to Advanced LIGO/VIRGO detectors, middle to ET detector and bottom to DECIGO detector. In first row of each table one can see the eccentricity where difference between number of orbits is in the order of 1 compared to circular case. Then we presented percent of binaries of different types (double neutron stars, black hole - neutron star and binary black hole) that has larger eccentricity than limit in first row. In brackets we put number of those systems. We listed results for all considered models.

30 Hz			
	NS-NS	BH-NS	BH-BH
$e(30 \text{ Hz})_{\text{lim}}$	1.35e-02	2.61e-02	6.98e-02
AZK	0.53% (45)	0.15% (1)	0.00% (0)
BZK	1.13% (32)	0.00% (0)	0.00% (0)
AZk	0.14% (24)	0.00% (0)	0.00% (0)
BZk	0.28% (14)	0.00% (0)	0.00% (0)
AzK	0.28% (24)	0.44% (11)	0.01% (2)
BzK	1.87% (13)	0.48% (7)	0.08% (1)
Azk	0.23% (33)	0.23% (10)	0.00% (0)
Bzk	1.57% (19)	0.25% (6)	0.00% (0)
3 Hz			
	NS-NS	BH-NS	BH-BH
$e(3 \text{ Hz})_{\text{lim}}$	1.89e-03	3.65e-03	9.76e-03
AZK	2.98% (253)	1.16% (8)	0.62% (2)
BZK	4.62% (131)	0.00% (0)	0.00% (0)
AZk	0.91% (152)	0.54% (7)	0.00% (0)
BZk	1.60% (79)	7.69% (1)	0.00% (0)
AzK	3.08% (266)	1.40% (35)	0.02% (4)
BzK	6.03% (42)	1.51% (22)	0.15% (2)
Azk	1.83% (259)	0.94% (41)	0.01% (2)
Bzk	5.55% (67)	1.12% (27)	0.05% (1)
0.3 Hz			
	NS-NS	BH-NS	BH-BH
$e(0.3 \text{ Hz})_{\text{lim}}$	2.64e-04	6.00e-04	1.36e-03
AZK	68.11% (5781)	15.99% (110)	2.49% (8)
BZK	48.38% (1373)	50.00% (1)	0.00% (0)
AZk	57.97% (9678)	3.00% (39)	2.16% (11)
BZk	26.34% (1303)	30.77% (4)	0.00% (0)
AzK	83.58% (7228)	13.55% (339)	0.39% (69)
BzK	54.52% (380)	15.61% (228)	3.23% (42)
Azk	74.78% (10556)	5.62% (244)	0.22% (44)
Bzk	36.79% (444)	4.15% (100)	0.29% (6)



**Table 4.** Percent of the compact binaries that should be detectable in future interferometers. Top table correspond to Advanced LIGO/VIRGO detectors, middle to ET detector and bottom to DECIGO detector. In first row of each table one can see the eccentricity where difference between number of orbits is in the order of 10 compared to circular case. Then we presented percent of binaries of different types (double neutron stars, black hole - neutron star and binary black hole) that has larger eccentricity than limit in first row. In brackets we put number of those systems. We listed results for all considered models.

30 Hz			
	NS-NS	BH-NS	BH-BH
$e(30 \text{ Hz})_{\text{lim}}$	4.27e-02	8.23e-02	2.20e-01
AZK	0.29% (25)	0.15% (1)	0.00%(0)
BZK	0.63% (18)	0.00% (0)	0.00%(0)
AZk	0.07% (12)	0.00% (0)	0.00%(0)
BZk	0.14% (7)	0.00% (0)	0.00%(0)
AzK	0.23% (20)	0.24% (6)	0.00%(0)
BzK	1.87% (13)	0.21% (3)	0.00%(0)
Azk	0.16% (23)	0.05% (2)	0.00%(0)
Bzk	1.24% (15)	0.00% (0)	0.00%(0)

3 Hz			
	NS-NS	BH-NS	BH-BH
$e(3 \text{ Hz})_{\text{lim}}$	5.96e-03	1.15e-02	3.08e-02
AZK	1.52% (129)	0.73% (5)	0.31%(1)
BZK	2.50% (71)	0.00% (0)	0.00%(0)
AZk	0.47% (78)	0.54% (7)	0.00%(0)
BZk	0.93% (46)	7.69% (1)	0.00%(0)
AzK	1.39% (120)	0.92% (23)	0.02%(3)
BzK	4.30% (30)	1.23% (18)	0.15%(2)
Azk	0.66% (93)	0.76% (33)	0.00%(1)
Bzk	3.89% (47)	0.87% (21)	0.00%(0)

0.3 Hz			
	NS-NS	BH-NS	BH-BH
$e(0.3 \text{ Hz})_{\text{lim}}$	8.33e-04	1.89e-03	4.30e-03
AZK	55.56% (4716)	6.69% (46)	2.18%(7)
BZK	26.36% (748)	50.00% (1)	0.00%(0)
AZk	50.02% (8351)	1.31% (17)	1.18%(6)
BZk	11.46% (567)	30.77% (4)	0.00%(0)
AzK	75.89% (6563)	7.39% (185)	0.22%(38)
BzK	22.09% (154)	7.67% (112)	1.08%(14)
Azk	69.38% (9795)	4.44% (193)	0.17%(34)
Bzk	19.55% (236)	2.69% (65)	0.29%(6)

**Table 5.** Percent of the compact binaries that should be detectable in future interferometers. Top table correspond to Advanced LIGO/VIRGO detectors, middle to ET detector and bottom to DECIGO detector. In first row of each table one can see the eccentricity where difference between number of orbits is in the order of 100 compared to circular case. Then we presented percent of binaries of different types (double neutron stars, black hole - neutron star and binary black hole) that has larger eccentricity than limit in first row. In brackets we put number of those systems. We listed results for all considered models.

30 Hz			
	NS-NS	BH-NS	BH-BH
$e(30 \text{ Hz})_{\text{lim}}$	1.35e-01	2.59e-01	1
AZK	0.14% (12)	0.15% (1)	0.00%(0)
BZK	0.21% (6)	0.00% (0)	0.00%(0)
AZk	0.03% (5)	0.00% (0)	0.00%(0)
BZk	0.06% (3)	0.00% (0)	0.00%(0)
AzK	0.16% (14)	0.12% (3)	0.00%(0)
BzK	1.72% (12)	0.21% (3)	0.00%(0)
Azk	0.11% (16)	0.05% (2)	0.00%(0)
Bzk	0.91% (11)	0.00% (0)	0.00%(0)

3 Hz			
	NS-NS	BH-NS	BH-BH
$e(3 \text{ Hz})_{\text{lim}}$	1.88e-02	3.62e-02	9.70e-02
AZK	1.05% (89)	0.44% (3)	0.31%(1)
BZK	1.97% (56)	0.00% (0)	0.00%(0)
AZk	0.30% (50)	0.38% (5)	0.00%(0)
BZk	0.59% (29)	0.00% (0)	0.00%(0)
AzK	0.68% (59)	0.72% (18)	0.02%(3)
BzK	3.16% (22)	0.96% (14)	0.15%(2)
Azk	0.47% (67)	0.55% (24)	0.00%(1)
Bzk	2.98% (36)	0.62% (15)	0.00%(0)

0.3 Hz			
	NS-NS	BH-NS	BH-BH
$e(0.3 \text{ Hz})_{\text{lim}}$	2.63e-03	5.96e-03	1.35e-02
AZK	41.26% (3502)	3.34% (23)	1.87%(6)
BZK	14.27% (405)	0.00% (0)	0.00%(0)
AZk	40.26% (6721)	0.69% (9)	0.20%(1)
BZk	4.83% (239)	15.38% (2)	0.00%(0)
AzK	68.63% (5935)	5.28% (132)	0.12%(21)
BzK	14.06% (98)	5.13% (75)	0.46%(6)
Azk	66.41% (9375)	3.73% (162)	0.02%(4)
Bzk	11.68% (141)	2.03% (49)	0.10%(2)

#### 4. Summary

We have presented the distributions of eccentricities of compact object binaries at three frequencies right before merger. The properties of the compact object binaries are calculated using the StarTrack population synthesis code. We find that the distributions of eccentricities of the compact object binaries do not depend strongly on the assumed model of binary evolution. The main dependence shows up in the case of binary neutron stars. For binary neutron star the distribution may be either single or double peaked. The extra peak corresponds to ultra-compact NS-NS binaries that have undergone an additional CE phase right before formation of the second NS. In order to make the results easier to use in the simulations we have fitted the resulting distributions of eccentricity with a model of a log-normal distribution:

$$f(x) = a \exp\left(-\frac{(x - \mu)^2}{2\sigma^2}\right) \quad (7)$$

where  $x = \log e$ ,  $a$  is normalization,  $\mu$  is mean and  $\sigma$  is variance.

In the case BH-BH and BH-NS binaries the distribution is modeled with a single log-normal distribution while in the case of the NS-NS eccentricities we used a sum of two log-normal distributions, since the distribution is double peaked. The results of the fits are shown in Table 6.

**Table 6.** Parameters of log normal distribution fitted to results of model AZK

NS-NS			
	0.3 Hz	3 Hz	30 Hz
$a_1$	$0.38 \pm 0.03$	$0.38 \pm 0.02$	$0.37 \pm 0.02$
$\mu_1$	$-3.78 \pm 0.04$	$-4.82 \pm 0.04$	$-5.87 \pm 0.04$
$\sigma_1$	$0.52 \pm 0.05$	$0.55 \pm 0.05$	$0.56 \pm 0.04$
$a_2$	$0.56 \pm 0.04$	$0.56 \pm 0.04$	$0.56 \pm 0.04$
$\mu_2$	$-2.34 \pm 0.03$	$-3.39 \pm 0.03$	$-4.44 \pm 0.03$
$\sigma_2$	$0.40 \pm 0.04$	$0.39 \pm 0.04$	$0.39 \pm 0.03$
BH-NS			
	0.3 Hz	3 Hz	30 Hz
$a$	$0.71 \pm 0.05$	$0.72 \pm 0.04$	$0.68 \pm 0.03$
$\mu$	$-4.18 \pm 0.04$	$-5.23 \pm 0.03$	$-6.27 \pm 0.03$
$\sigma$	$0.51 \pm 0.04$	$0.51 \pm 0.03$	$0.55 \pm 0.03$
BH-BH			
	0.3 Hz	3 Hz	30 Hz
$a$	$0.61 \pm 0.06$	$0.61 \pm 0.02$	$0.60 \pm 0.02$
$\mu$	$-4.91 \pm 0.08$	$-5.95 \pm 0.03$	$-7.06 \pm 0.03$
$\sigma$	$0.67 \pm 0.08$	$0.65 \pm 0.03$	$0.70 \pm 0.03$

The eccentricity of BH-BH binaries in all three cases is negligible. This is due to two factors. First, at the frequencies of interest the BH-BH systems are much closer to coalescence than the neutron star. Second the initial kicks at formation of BHs are lower than in the case of NS, so typically the initial eccentricities of BH-BH systems are lower than in the case NS-NS ones.

The eccentricities of the mixed BH-NS systems are larger than in the case of BH-BH ones. However, the number of systems with detectable eccentricity is small enough so that neglecting eccentricity will not decrease the sensitivity of Advanced LIGO/VIRGO detectors. However in the case of ET-like detector some eccentric systems may be detected. In the case of DECIGO like detector the number of detectable eccentric system will be somewhere between a few and a few tens percent.

The eccentricity of NS-NS systems are larger than those of binaries containing BHs. Yet in the case of Advanced LIGO/VIRGO detectors an assumption of circular orbit is very well justified and we expected less than 2% of binaries with marginally detectable eccentricity. In the case of ET this fraction is still small but can reach 6%. Given a much larger expected detection rate for ET this means that there should be a significant number of NS-NS binaries with detectable eccentricity. Finally in the case of DECIGO a significant number of binaries will have detectable eccentricity. This fraction can reach even 70%. Moreover, the shape of the distribution eccentricity of NS-NS binaries will depend on the existence of the evolutionary scenario that leads to formation of ultra-compact binaries.

To check if binaries with significant eccentricity would be seen in Advanced LIGO/VIRGO detectors we compare our results with detection rate predictions. Table 7 presents product of detection rate from Table V of Abadie et al. (2010) and the fraction percent of binaries with detectable eccentricity taken from Table 3. We present the results using the pessimistic case and the optimistic one in brackets. This shows that there is a chance of detecting eccentric binaries already with the Advanced LIGO/VIRGO detectors provided that the rates are not the pessimistic ones. Depending on model we can expect from  $\approx 50$  to  $\approx 700$  NS-NS coalescence detections per year assuming optimistic predictions. For mixed binaries (BH-NS) number of expected events per year reaches  $\approx 140$ . In the case of BH-BH we don't expect any detection of eccentric binary, except from two models (AzK and BzK) with low metallicity.

**Table 7.** Number of interesting events per year expected to seen in Advanced LIGO/VIRGO. First number assumes low detection rate and number in brackets assumes high detection rate given by Abadie et al. (2010, Table V)

30 Hz			
	NS-NS	BH-NS	BH-BH
AZK	0.212 (212.0)	0.030 (45.0)	0.000 (0.0)
BZK	0.452 (452.0)	0.000 (0.0)	0.000 (0.0)
AZk	0.056 (56.0)	0.000 (0.0)	0.000 (0.0)
BZk	0.112 (112.0)	0.000 (0.0)	0.000 (0.0)
AzK	0.112 (112.0)	0.088 (132.0)	0.004 (10.0)
BzK	0.748 (748.0)	0.096 (144.0)	0.032 (80.0)
Azk	0.092 (92.0)	0.046 (69.0)	0.000 (0.0)
Bzk	0.628 (628.0)	0.050 (75.0)	0.000 (0.0)

In reality for each detector the low frequency cutoff is not so sharp, and a given binary shall become detectable at different frequency depending on the distance, however in this paper we are aiming at understanding the basic trends and we assume that we can model the sensitivity curves of the detectors with rough cutoffs at low frequency.

#### Acknowledgments

This work was supported by the EGO-DIR-102-2007; the FOCUS 4/2007 Program of Foundation for Polish Science, the Polish grants N N203 511238, DPN/N176/VIRGO/2009, N N203 302835, N N203 404939 and by CompStar a Research Networking Programme of the European Science Foundation.

## References

- Abadie, J., Abbott, B. P., Abbott, R., et al. 2010, *Classical and Quantum Gravity*, 27, 173001
- Acernese, F., Amico, P., Al-Shourbagy, M., et al. 2006, *Classical and Quantum Gravity*, 23, 63
- Anderson, S. B., Gorham, P. W., Kulkarni, S. R., Prince, T. A., & Wolszczan, A. 1990, *Nature*, 346, 42
- Belczynski, K., Bulik, T., Fryer, C. L., et al. 2010a, *ApJ*, 714, 1217
- Belczynski, K., Bulik, T., & Kalogera, V. 2002a, *ApJ*, 571, L147
- Belczynski, K., Dominik, M., Bulik, T., et al. 2010b, *ApJ*, 715, L138
- Belczynski, K., Kalogera, V., & Bulik, T. 2002b, *ApJ*, 572, 407
- Belczynski, K., Kalogera, V., Rasio, F. A., et al. 2008, *ApJS*, 174, 223
- Belczynski, K., Taam, R. E., Kalogera, V., Rasio, F. A., & Bulik, T. 2007, *ApJ*, 662, 504
- Bogomazov, A. I., Lipunov, V. M., & Tutukov, A. V. 2007, *Astronomy Reports*, 51, 308
- Brown, D. A. & Zimmerman, P. J. 2010, *Phys. Rev. D*, 81, 024007
- Burgay, M., D'Amico, N., Possenti, A., et al. 2003, *Nature*, 426, 531
- Cokelaer, T. & Pathak, D. 2009, *Classical and Quantum Gravity*, 26, 045013
- De Donder, E. & Vanbeveren, D. 2004, *New A*, 9, 1
- Dessart, L., Burrows, A., Ott, C. D., et al. 2006, *ApJ*, 644, 1063
- Dewi, J. D. M., Podsiadlowski, P., & Pols, O. R. 2005, *MNRAS*, 363, L71
- Dewi, J. D. M., Pols, O. R., Savonije, G. J., & van den Heuvel, E. P. J. 2002, *MNRAS*, 331, 1027
- Faulkner, A. J., Kramer, M., Lyne, A. G., et al. 2005, *ApJ*, 618, L119
- Fryer, C. L. & Kalogera, V. 2001, *ApJ*, 554, 548
- Gondek-Rosińska, D., Bulik, T., & Belczyński, K. 2007, *Advances in Space Research*, 39, 285
- Harry, G. M. & the LIGO Scientific Collaboration. 2010, *Classical and Quantum Gravity*, 27, 084006
- Hobbs, G., Lorimer, D. R., Lyne, A. G., & Kramer, M. 2005, *MNRAS*, 360, 974
- Hut, P. 1981, *A&A*, 99, 126
- Ivanova, N. & Taam, R. E. 2004, *ApJ*, 601, 1058
- Kawamura, S. 2006, *Astronomical Herald*, 99, 490
- Kiel, P. D., Hurley, J. R., & Bailes, M. 2010, *MNRAS*, 406, 656
- Kitaura, F. S., Janka, H., & Hillebrandt, W. 2006, *A&A*, 450, 345
- Lorimer, D. R., Stairs, I. H., Freire, P. C., et al. 2006, *ApJ*, 640, 428
- Mandel, I. & O'Shaughnessy, R. 2010, *Classical and Quantum Gravity*, 27, 114007
- Nelemans, G. & van den Heuvel, E. P. J. 2001, *A&A*, 376, 950
- Peters, P. C. 1964, *Physical Review*, 136, 1224
- Peters, P. C. & Mathews, J. 1963, *Physical Review*, 131, 435
- Pfahl, E., Podsiadlowski, P., & Rappaport, S. 2005, *ApJ*, 628, 343
- Schnittman, J. D. 2004, *Phys. Rev. D*, 70, 124020
- Seto, N., Kawamura, S., & Nakamura, T. 2001, *Physical Review Letters*, 87, 221103
- Sipior, M. S. & Sigurdsson, S. 2002, *ApJ*, 572, 962
- Smith, J. R. & LIGO Scientific Collaboration. 2009, *Classical and Quantum Gravity*, 26, 114013
- Spallicci, A. D. A. M., Aoudia, S., de Freitas Pacheco, J., Regimbau, T., & Frossati, G. 2005, *Classical and Quantum Gravity*, 22, 461
- Taam, R. E. & Sandquist, E. L. 2000, *ARA&A*, 38, 113
- Timmes, F. X., Woosley, S. E., & Weaver, T. A. 1996, *ApJ*, 457, 834
- Van Den Broeck, C. 2010, *ArXiv e-prints*
- Voss, R. & Tauris, T. M. 2003, *MNRAS*, 342, 1169
- Webbink, R. F. 1984, *ApJ*, 277, 355
- Weisberg, J. M. & Taylor, J. H. 2005, in *Astronomical Society of the Pacific Conference Series*, Vol. 328, *Binary Radio Pulsars*, ed. F. A. Rasio & I. H. Stairs, 25–+
- Wolszczan, A. 1991, *Nature*, 350, 688